Interference power statistics in ad-hoc and sensor networks

R. Hekmat · P. Van Mieghem

Abstract There exist accurate calculation methods for estimation of interference power sum statistics in fixed-topology wireless networks based on the log-normal shadowing radio model. Here we publish essential additions to these estimation methods to expand their use to sensor networks and ad-hoc networks with changing topology. In our calculations we take into account radio propagation conditions, density of nodes, size of the network, traffic load per node and MAC protocol characteristics. The accuracy of our calculation method is verified by simulations. We highlight the influence of MAC protocols on interference and show that an increase in network size or in node density does not necessarily lead into higher interference values. Our results can be deployed to estimate the network capacity.

Keywords Ad-hoc networks · Interference estimation · Radio model · MAC · Capacity · Network topology

1 Introduction

For performance evaluation and determination of the capacity in any wireless network it is important to have good calculation models to estimate interference statistics. These models already exist for fixed topology networks like cellular networks (see e.g. [7]). For ad-hoc and sensor networks, only the "order of magnitude" of interference and network

R. Hekmat (✉) · P. Van Mieghem
Delft University of Technology, Electrical Engineering,
Mathematics and Computer Science, P.O. Box 5031,
2600 GA Delft, The Netherlands
e-mail: R.Hekmat@ewi.tudelft.nl

P. Van Mieghem
e-mail: P.VanMieghem@ewi.tudelft.nl

capacity have already received attention (see e.g. [8] and [5]). However, to our best knowledge, till now there has been no accurate calculation model to estimate the expected interference power and its distribution function in ad-hoc and sensor networks. In this paper we have used the method for estimation of interference statistics in fixed topology networks and have added required features to enable us to calculate with good accuracy interference power statistics in wireless ad-hoc and sensor networks. Our interference calculation model takes into account radio propagation conditions, density of nodes, size of the network, MAC protocol characteristics and traffic load per node. The accuracy of our approach has been verified by simulations.

The structure of this paper is as follows. In Section 2 we explain briefly the log-normal radio propagation model which is used in our interference calculations. Section 3 illustrates how the MAC protocol restricts the interfering node density, and consequently the interference power sum. In Section 4 we describe two important aspects specific to ad-hoc and sensor networks that should be taken into account for correct estimation of the interference power sum. Conclusions are summarized in Section 5.

2 The radio model

The most commonly used radio model for the study of ad-hoc networks is the so-called pathloss model. This model assumes that the received signal power at distance r is equal to $c \cdot r^{-\eta}$, where c is a constant and η is the pathloss exponent. The pathloss exponent depends on the environment and terrain structure and can vary between 2 in free space to 6 in heavily built urban areas [15]. We will call the signal power at distance r predicted by the pathloss model the *area mean power*. Assume radio signals can be received correctly when
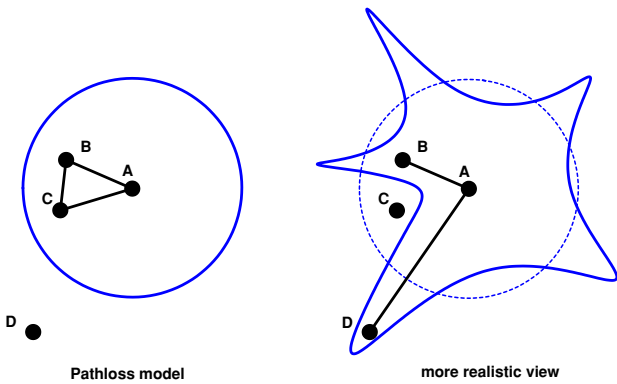
Fig. 1 Schematic view showing the nondeterministic nature of radio links where short distance links may not exist while long distance links do

Fig. 2 Link probability with log-normal shadowing radio model for some ξ values. In the case $\xi = 0$ the log-normal model reduces to the pathloss model with circular coverage per node

their power exceeds a minimum threshold value γ. With this assumption, the pathloss model results into a perfect circular coverage area around each node with radius $R = (c/\gamma)^{1/\eta}$. However, this is an unrealistic assumption in most practical situations. In reality the received power levels may show significant variations around the area mean power. Due to these variations, the coverage area will deviate from a perfect circular shape and consequently, some short links could disappear while long links could emerge (see Fig. 1).

The log-normal radio model that we use in this paper is more realistic than the pathloss model because it allows for random signal power variations. The motivation for using the log-normal radio model in ad-hoc networks is given in [4], [10] and [11]. The log-normal radio model assumes that the logarithmic value of the received signal power at distance r is normally distributed with standard deviation σ around the logarithm of the area mean power. The magnitude of the standard deviation indicates the severity of signal fluctuations caused by irregularities in the surroundings of the receiving and transmitting antennas. For convenience of notation we normalize all distances to R and all powers to γ. According to the log-normal radio model, the normalized received power, $\widehat{\mathbf{P}}$, at normalized distance $\widehat{r} \triangleq r/R$ can be written as [10]:

$$10 \log_{10} \widehat{\mathbf{P}}(\widehat{r}) = 10 \log_{10} \left(\widehat{r}^{-\eta} \right) + x \qquad (1)$$

where x is a zero-mean normal distributed random variable (in dB) with standard deviation σ (also in dB). The condition for correct reception of signals at normalized distance $\widehat{r}$ is that the normalized power at this distance is more than 1 (or zero dB). Based on the log-normal shadowing radio model the probability that two nodes are connected (link probability) is [11]:

$$p(\widehat{r}) = \frac{1}{2} \left[1 - \mathrm{erf} \left(\alpha \frac{\log(\widehat{r})}{\xi} \right) \right], \quad \xi \triangleq \sigma/\eta \qquad (2)$$
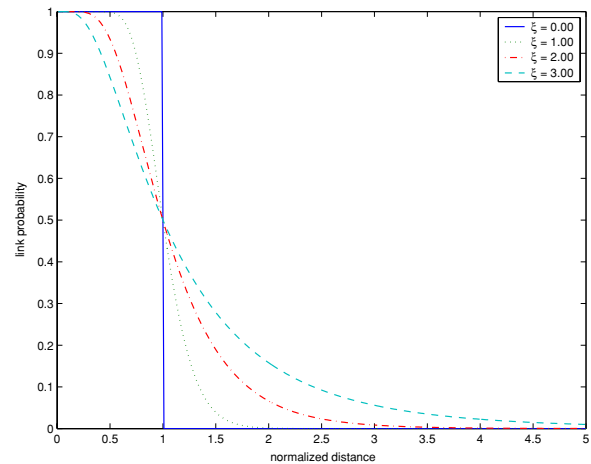
where $\alpha = 10/(\sqrt{2} \log 10)$, and ξ is defined as the ratio between the standard deviation of shadowing, σ, and the pathloss exponent, η. Low values of ξ correspond to small variations of the signal power around the area mean power and high values of ξ correspond to stronger shadowing effects. In [11] is indicated that in theory ξ may vary between 0 and 6, although values higher than 3 seem to be unrealistic.[1] In the case of $\xi \rightarrow 0$, there is no shadowing effect and our model is equivalent to the pathloss model (a simple step function):

$$\lim_{\xi \to 0} p(\widehat{r}) = \begin{cases} 1 & \text{if} \quad \widehat{r} < 1 \\ 0 & \text{if} \quad \widehat{r} > 1 \end{cases}.$$

Figure 2 shows the link probability for some values of ξ.

3 Effect of the MAC protocol on the interfering node density

Medium Access Control (MAC) protocols restrict the number of simultaneous signal transmissions per unit of area and consequently curb the aggregate interference power in ad-hoc networks. Many papers have been published about MAC protocols for ad-hoc networks. It is beyond the scope of this paper to describe them. However, as depicted in Fig. 3, MAC protocols can be classified into three distinct classes based on the method that they handle hidden and

---

[1] The pathloss exponent η can vary between 2 in free space to 6 in heavily built urban areas. Measurements [15] have shown that σ could vary between 0 and 12. However, high values of σ correspond with heavily built and irregular areas where the pathloss exponent is high as well. This clarifies our statement that ξ values higher than 3 are unrealistic.
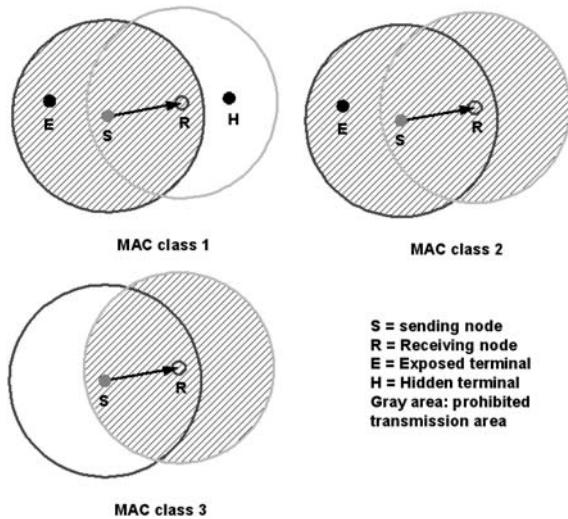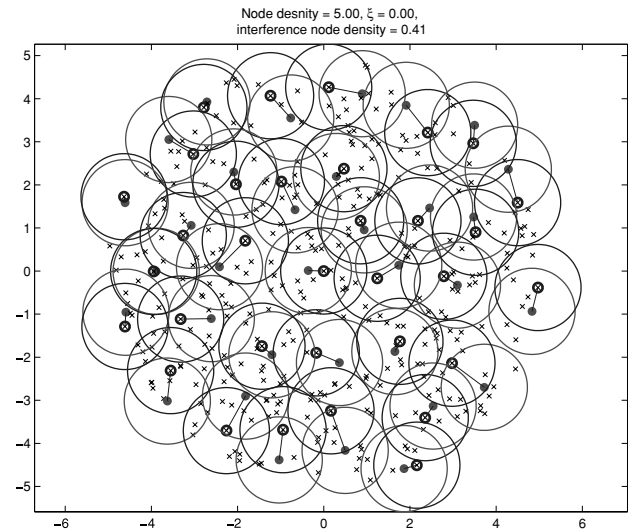
Fig. 3 Schematic view showing the working of three MAC classes. In this figure, for simplicity, we have assumed circular coverage area for each node ($\xi = 0$)

Fig. 4 The working of MAC class 2 on randomly distributed nodes in a circular area with $\xi = 0$. Nodes indicated by $\times$ sign are prohibited form transmission

exposed node problems (for a description of hidden and exposed node problems see e.g. [18]):

Class 1: The MAC protocol prohibits simultaneous transmissions within the sender's radio range. This class leaves the hidden node as well as exposed node problem unsolved. CSMA/CA without reservation [1] is a typical example of MAC protocols that fall into this category.

Class 2: The MAC protocol prohibits simultaneous transmissions within the sender's as well as receiver's radio range. This class solves the hidden node problem but leaves the exposed node problem unsolved. CSMA/CA with reservation [1] is an example of this category. Other examples are MARCH [17] and S-MAC [19].

Class 3: The MAC protocol prohibits simultaneous transmissions within the receivers's radio range and simultaneous transmissions towards nodes within the sender's radio range. This class solves both the hidden node as well as exposed node problems, but requires e.g. the deployment of an additional signalling channel. Two MAC protocols

that fall into this category are RBCS [12] and DBTMA [9].

This method of classification is based on the way that a MAC protocol allows or prohibits nodes in the coverage area of nodes **S** and **R** to send or receive data while a packed is being transmitted from node **S** to node **R**. Figure 3 gives a schematic view but does not show the details regarding nodes being able either to send data to or receive data from other nodes. A more detailed description of the operation of the three MAC protocol classes is given in Table 1.

Figure 4 shows the prohibited areas with circles around the sending and receiving nodes for an example of MAC class 2.

For the calculation of the interference power in ad-hoc and sensor networks the density and the distribution of interfering nodes must be known. When the density of nodes increases, more nodes will fall within prohibited transmission areas. As a result, the density of interfering nodes is not

Table 1 Prohibited and allowed transmission/reception possibilities for different classes of the MAC protocols

	Nodes inside **S** but outside **R** coverage (denoted as **E**)		Nodes inside **R** but outside **S** coverage (denoted as **H**)		Nodes in overlapping **S** and **R** coverage	
	May send	May receive	May send	May receive	May send	May receive
MAC class 1	no (1)	yes (2)	yes (3)	yes (4)	no	yes (2)
MAC class 2	no (1)	no (5)	no	no	no	no
MAC class 3	yes (6)	no	no	yes (7)	no	no

1: This could have been allowed as long as destination node is outside the coverage area of **R**.
2: From nodes outside the coverage area of node **S**.
3: To any node.
4: From nodes outside the coverage area of node **S**.
5: If **E** was allowed to receive, the packet intended for it would have collided with data coming from **S**.
6: To nodes outside the coverage area of node **R**.
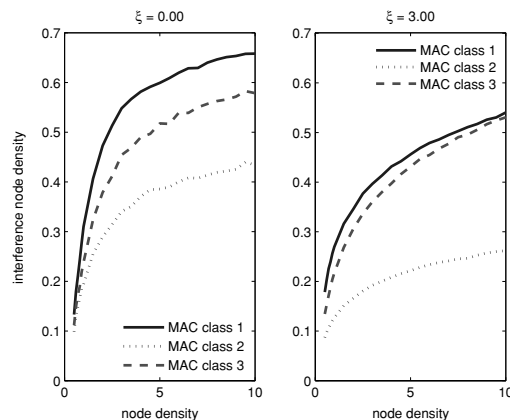7: From nodes outside the coverage area of **R**.
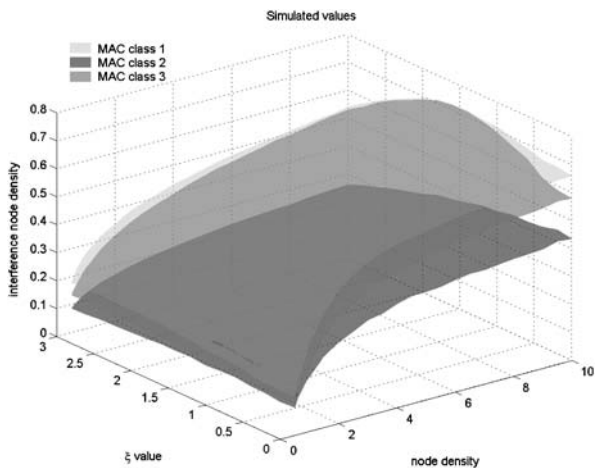
Fig. 5 Density of interfering nodes found by simulations for MAC classes 1, 2 and 3 ($0 \leq \xi \leq 3$ and $0.5 \leq \rho \leq 10$)

Fig. 6 Density of interfering nodes found by simulations for MAC classes 1, 2 and 3. Left subplot: $0.5 \leq \rho \leq 10$ and $\xi = 0$, right subplot: $0.5 \leq \rho \leq 10$ and $\xi = 3$

expected to increase linearly with the increase in the density of nodes.

We argue here that the interfering node density, ν, depends not only on the density of nodes forming the network, ρ, but also on the MAC protocol class and the radio propagation factor ξ (explained in Section 2). ξ determines the link probability between nodes and consequently the shape and the extent of the coverage area around each node. For a wide range of ξ and ρ values we have performed simulations to find the interfering node density for each MAC class. In each simulation case we have placed one receiving node in the center of a sufficiently large circular area.[2] Other nodes are uniformly distributed over this area with a given density. Then we form sending-receiving node pairs by taking MAC protocol restrictions into account and assuming that nodes always have data to send to any of their neighbours (activity ratio 100%). The number of sending nodes found in this way determines the interfering node density. Simulation results are shown in Fig. 5. For better inspection of results a part of the simulation data is redrawn in Fig. 6. It can be seen from these figures that, as expected, the interfering node density is highest in MAC class 1 and lowest in MAC class 2, with MAC class 3 in-between. We see also that when the node density ρ increases, the interfering node density ν increases as well but tends to level off for large values of ρ. In fact in our simulations the interfering node density always remains under 0.8. Further, because the average node degree (neighbors per node) depends on ξ, the interfering node density depends on ξ as well. By increasing ξ the average node degree increases [10], thus for each sending-receiving pair

formed, the number of nodes falling within the prohibited transmission areas increases as well. Therefore, as observed in Fig. 6, the number of potential interfering nodes tends to decrease[3] for the highest values of ξ in comparison to the case $\xi = 0$.

Using simulation results, we have found two-dimensional fitting formulas for the interfering node density:

$$\nu \simeq \begin{cases} 0.3466 + 0.1658 \log(\rho) - 0.0283\xi & \text{MAC class 1} \\ 0.2403 + 0.0910 \log(\rho) - 0.0453\xi & \text{MAC class 2} \\ 0.2634 + 0.1741 \log(\rho) - 0.0130\xi & \text{MAC class 3} \end{cases}$$

$$(3)$$

where $0.5 \leq \rho \leq 10$ and $0 \leq \xi \leq 3$. The root-mean-square error in the fit is 0.04, 0.02 and 0.03 for, respectively, MAC classes 1, 2 and 3.

Based on (3) we may conclude that ν is by approximation a linear function of $\log(\rho)$ for the range of ρ values included in our simulations.[4] Figure 7 shows the interfering nodes densities calculated using (3).

---

[2] In our simulations the normalized radius of the circular area has been set to 3 times the distance where the link probability (2) drops to 5%. Therefore, the normalized radius of the area depends on the factor ξ. As an example, the normalized radius of the simulation area is 9.6 in case of $\xi = 3$, in other words 9.6 times the distance R defined in Section 2.

[3] To be precise, our simulations have shown situations where by changing ξ from 0 to 3 the interfering node density increases slightly at first before starting to decease. This only happens for MAC classes 1 and 3 at high values of ρ (notice the slight bending of the interfering node density for MAC class 1 and 3 at $\rho = 10$ in Fig. 5). The explanation for this effect is that in MAC classes 1 and 3, in contrast to MAC class 2, a node inside the prohibited areas still may receive data from nodes outside these areas. When ξ increases the number of nodes that fall inside the prohibited areas increases as well. On one hand this increases the number of potential receivers and makes new sending-receiving node pair combinations possible. On the other hand, for each sending-receiving pair formed, the number of nodes not allowed to send increases. Simulations seem to indicate that the combined outcome of these two effects is the decrease of interfering node density for the highest values of ξ.

[4] As mentioned above, due to the working of MAC protocols, ν is expected to level off for large values of ρ. In other words we expect that ν would asymptotically approach a constant.
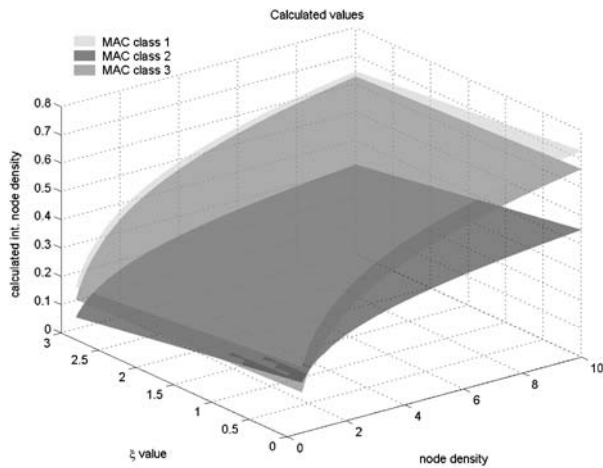
Fig. 7 Estimated interfering nodes densities using (3) for MAC classes 1, 2 and 3

As mentioned before our simulations are based on the assumption that all nodes in the ad-hoc or the sensor network always have data to send to any of their neighbours. In reality this is not the case. At any moment in time only a portion of nodes forming the network are active. If the activity ratio is indicated by a, we can use (3) to estimate the interfering node density by replacing ρ with $a\rho$.

4 Interference power estimation

As described in Section 2 we are assuming log-normal distributed powers, which implies that the interference consists of log-normal components. The sum of log-normal components is a well-studied topic in cellular networks (see e.g. [14]). Although an exact analytic expression has not been found for the power sum of log-normal components in general, there exist two widely accepted good approximation methods. The first method is Fenton-Wilkinson (WF) approximation [3, 6], . The second method is Schwartz-Yeh (SY) approximation [16]. Both methods assume that the power sum of log-normal components has a log-normal distribution with a mean and a variance that can be calculated directly from the mean and the variance of each individual component (and if applicable, the correlation factor between the components).

In this paper we expand these approximation methods, to our best knowledge for the first time, to estimate the sum of interference powers in ad-hoc and sensor networks. Using (3) we can estimate the number of interfering components. The variance of log-normal interference components, σ^2, is a characteristic feature of the propagation environment and is given. However, the challenge in using these approximation methods for ad-hoc networks lies in estimating the

mean power of each individual component. This task is not trivial due to the following two reasons:

1. The mean interference power experienced at node i from node j is directly linked to the distance between i and j. Because of the random distribution and the movement of nodes this distance is subject to changes. In Section 4.1 we describe a method to find the expected position of interfering nodes.

2. Because of shadowing, for any fixed distance d_{ij} between nodes i and j there is a statistical probability that these two nodes are "visible" to each other (see link probability in Fig. 2). If node j is visible to node i, depending on the MAC protocol, it may be prohibited[5] from interfering with node i. This phenomenon, which does not exist in cellular networks, implies that knowing the distance to an interfering node (that provides us with the mean expected power coming from that node) and the variance of the interfering signal components is not enough to make an accurate estimation of the aggregate interference power. In Section 4.2 we provide a solution for this point.

4.1 Position of interfering nodes

Let us assume that interfering nodes are uniformly distributed with density ν around a center node in a circular area. We order these nodes according to their distance, r_m, to the center node. In other words, r_1 is the distance of the nearest interfering node to the center, r_2 denotes the distance of the second nearest interfering node to the center, and etc. The statistical probability function of the radius r_m of the m-th nearest interfering node to the center is [13]:

$$f_{r_m}(r) = \frac{2\pi r \nu}{(m-1)!} \left(\pi r^2 \nu\right)^{m-1} e^{-\pi r^2 \nu} \quad x, \quad m = 1, 2, 3, \dots$$
(4)

The expected distance of the m-th interfering node to the center node is then:

$$E[r_m] = \int_0^\infty r \, f_{r_m}(r) \, dr = \frac{\Gamma\left(m + \frac{1}{2}\right)}{\sqrt{\pi \nu}(m-1)!}.$$
(5)

Other moments of r_m are derived in the Appendix. In our calculations of interference power sums we can use (5) to estimate the expected distance of each interfering node to the center node. In other words, we have assumed that interfering nodes have a uniform distribution around the center node. The validity of this assumption is verified by simulations. Figure 8 shows an example for a network with node

---

[5] It is realistic to assume that MAC protocol is fast enough to catch up with medium scale power variations due to shadowing.
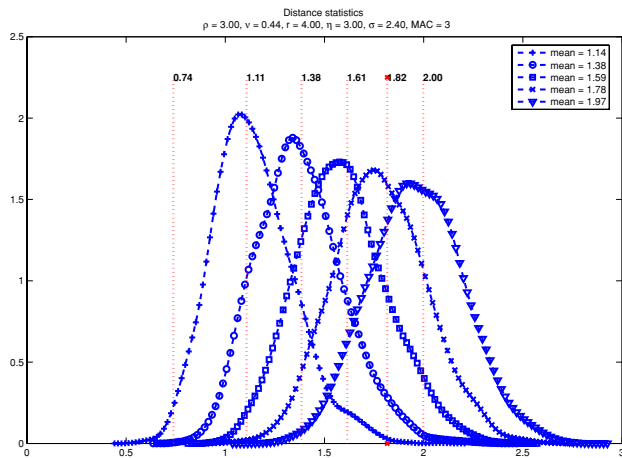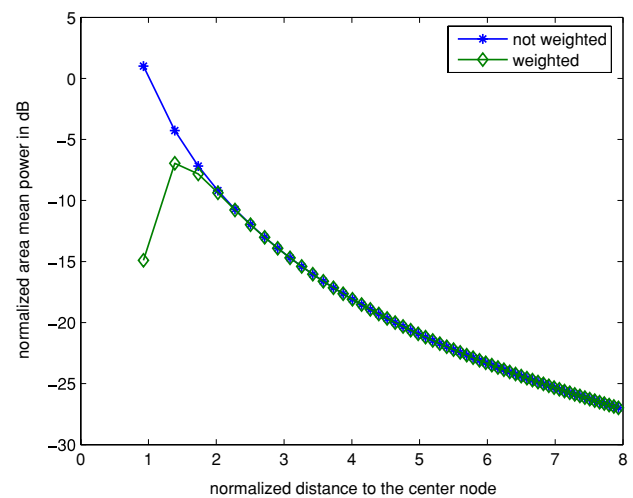
Fig. 8 Calculated distances of interfering nodes to the center node and simulated distribution of the distance of interfering nodes to the center node in an ad-hoc network with $r = 4$, $\rho = 3$, $\eta = 3$, $\sigma = 2.4$ and MAC class 3

density 3.0, pathloss exponent $\eta = 3.0$ and $\sigma = 2.4$. This results into an interfering node density of 0.44 (with MAC class 3 and $\xi = 0.8$). In this figure the dotted vertical lines indicate the distance of the first to the 6th interfering node calculated by (5). The marked curves show the actual distribution of the position of interfering nodes that are found by simulations. As we can see there is a very good match between the expected position (mean values) of interfering nodes found through simulations and the second to the 6th calculated values. However, (5) predicts an interfering node at distance 0.72 to the center node (the left most dotted vertical line in Fig. 8) that never seems to appear in simulations. The explanation is that a node at distance 0.72 would be connected to the center node with high probability.[6] Due to MAC class 3 restrictions this node is then not allowed to transmit a signal while the center node is receiving data from an other node. Therefore, assuming an interference power originated from this distance would provide erroneous results. This matter which is related to point 2 mentioned in the beginning of this section is dealt with by weighting the interference powers. The weighting method is described in the next section.

4.2 Weighting of interference mean powers

As mentioned above, in ad-hoc and sensor networks for any interfering node m at distance r_m there is a statistical probability that it is excluded from the power sum of interference power. This probability is proportional to the link probability $p(r_m)$, given by (2).

---

[6] The exact probability is calculated using (2): With $\xi = 2.4/3.0 = 0.8$ we obtain $p(\hat{r}) = 0.95$.

Fig. 9 Expected distance of interfering nodes to the center node and weighted as well as non-weighted area mean power expected from those distances in an ad-hoc network with MAC class 2, $r = 8$, $\rho = 3$, $\eta = 3.0$, $\sigma = 4.0$. The number of interfering nodes is 58 ($\nu = 0.28$)

In order to take this effect into account in the estimation of interference power sum, we suggest to weight the mean power of the m-th interfering signal with a factor proportional to $1 - p(r_m)$. Heuristically we have found out that a weight factor $w = (1 - p(r_m))^\sigma$ provides the best results. This weight factor takes into account not only the probability of the node being prohibited from transmission, but also the severity of shadowing represented by σ. The weight factor w varies between 0 and 1. As r_m increases $p(r_m)$ decreases, causing the weight factor to tend towards 1. At short distances the opposite occurs.

Figure 9 shows an example with the weighted and non-weighted area mean powers. We see that at short distances the weighting procedure reduces the strength of interfering signals (as in reality the MAC protocol would have done by not allowing strong interference from short distances) while at long distances there is no difference between the weighted and the non-weighted case.

4.3 Interference calculation results

Using our proposed method to find the distance of interfering nodes and the weighted mean power of individual interfering signals we are now ready to calculate the distribution function of interference power sum. The input parameters are the area size (circular area with normalized radius r), node density ρ, pathloss exponent η, shadowing standard deviation σ and the MAC protocol class. In this section we present our calculated values in a few representative examples and compare them with simulated results to verify the

accuracy of our calculation method. The calculation procedure is as follows:

1. The interfering node density is estimated using (3).
2. The expected positions of interfering nodes are found using (5).
3. The mean value of interference power coming from each interference source is weighted as described in Section 4.2.
4. The aggregate interference mean power and variance is estimated using the WF or SY method.[7]
5. The distribution function of the interference power is derived from the mean and the variance values assuming a log-normal distribution for the power sum.

The simulation procedure is:

1. Nodes are randomly distributed over a circular area with radius r and density ρ.
2. Sending and receiving node pairs are formed taking MAC protocol restrictions into account. In our simulations we have assumed that nodes always have data to send to any other neighbours.[8]
3. Each individual interference component is found using the log-normal propagation model (see (1)).
4. The aggregate interference power experienced at the center is obtained by adding all individual interference components.
5. To obtain the distribution function of the interference power the above steps have been repeated 1000 times.

We need to point out here that the calculation procedure stated above is very fast. The most computational extensive part of the calculation procedure is the WF or SY method. However, on a personal computer it takes only a few seconds to go through the calculation procedure. The simulation procedure however, depending on the radius of the coverage area and node density, can last several hours.

Figure 10 shows one set of results. Other results[9] are shown in Table 2. Note that the interference power values shown here are all **normalized** values according to the convention described in Section 2. Based on these results we argue that our calculation method is accurate in estimating

---

[7] WF method is more accurate when $\sigma \leq 4$ and SY method is more accurate when $\sigma > 4$. Both estimation methods are very fast as they consist of a set of closed mathematical expressions. Details of WF or SY estimation methods are beyond the scope of this paper. We refer to the provided references.

[8] This 100% activity assumption for nodes can be considered as a worst-case interference scenario. If the activity ratio of nodes is less than 1, our simulation as well as calculation method still can be used by multiplying the node density with the activity ratio.

[9] We have not presented any simulation results for MAC class 1, becuase due to the hidden node problem in this MAC class the interference power can explode.
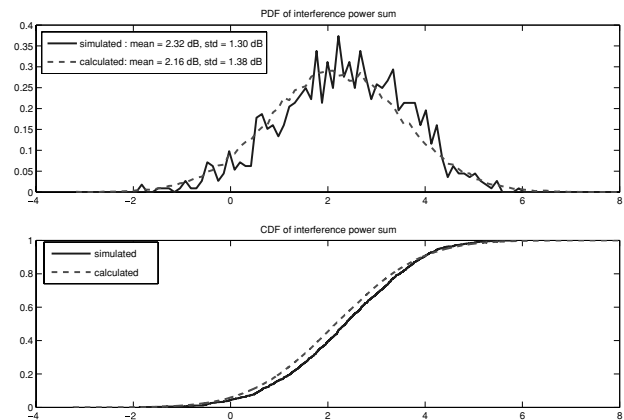
Fig. 10 Simulated and calculated PDF and CDF of normalized interference power in the center of a circular area with the same parameters as in Fig. 9
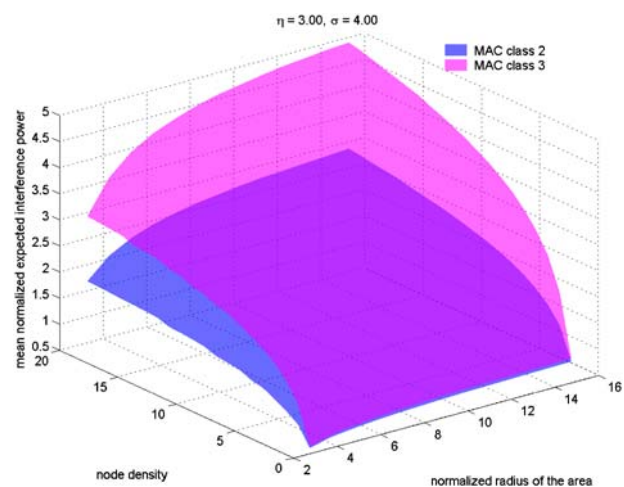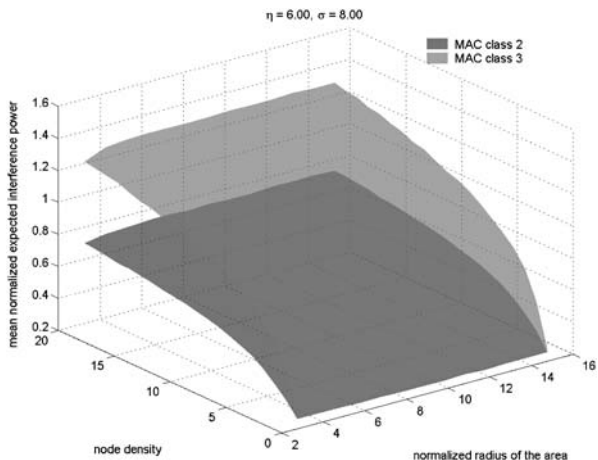

Fig. 11 Expected mean interference power as function of the network node density and area size for $\eta = 3.0$ and $\sigma = 4.0$

the mean interference signal powers especially in situations where interference is not weak. The standard deviation of interference power is estimated with less accuracy. This is due to the spreading of the actual position of interfering nodes around their expected position (see Fig. 8) which is not included in to our model yet. The variance of r_m for low values of ν is not negligible, as it has been shown in the Appendix.

Using our calculation method, we have plotted in Figs. 11 and 12 two examples of the mean normalized interference power sum as function of the area size and the node density. As we see, interference tends to level off when the node density or the area size increases. In other words, in ad-hoc and sensor networks increasing the area size or the node density does not necessarily imply an unacceptable increase in interference power. We also notice by comparing Figs. 11 and 12 that, as expected, the interference power is lower for a higher values of the pathloss exponent η.

Table 2 Calculated and simulated interference power statistics for several values of area radius r, node density ρ, pathloss exponent η, standard deviation of shadowing σ and MAC classes 2 and 3

Parameters	sim. mean (dB)	calc. mean (dB)	sim. std (dB)	calc. std (dB)
$r = 4.0, \rho = 8.0, \eta = 3.0, \sigma = 2.0$, MAC 2	2.78	2.76	1.10	0.76
$r = 6.0, \rho = 5.0, \eta = 2.4, \sigma = 1.5$, MAC 3	6.84	6.45	0.68	0.35
$r = 10.0, \rho = 1.0, \eta = 4.0, \sigma = 4.0$, MAC 2	−2.82	−2.31	2.57	2.13
$r = 8.0, \rho = 3.0, \eta = 4.0, \sigma = 9.0$, MAC 3	3.40	3.04	1.62	2.59
$r = 7.0, \rho = 3.0, \eta = 2.5, \sigma \approx 0$, MAC 3	5.71	5.57	0.63	0.00

Fig. 12 Expected mean interference power as function of the network node density and area size for $\eta = 6.0$ and $\sigma = 8.0$

The interference calculation method presented here can be used to estimate the capacity of ad-hoc and sensor networks.

5 Conclusions

The focus of this paper is on the estimation of interference power statistics in ad-hoc and sensor networks. First we have shown that the interfering node density depends on the MAC protocol characteristics. Each MAC protocol class restricts in its own way the number of interfering signal transmissions allowed per unit of area, regardless of the number of nodes falling within that area. Therefore, the interfering node density does not increase linearly with the density of nodes forming the network. In Section 3 we have found approximative formulas for calculating the expected interfering node density.

As main result of this paper we have presented a calculation method using log-normal radio propagation model for estimation of interference power sum statistics in ad-hoc and sensor networks. The input parameters for the model are the area size, density of the nodes, the radio propagation conditions (pathloss exponent and shadowing standard deviation), the activity ratio of nodes and MAC protocol characteristics.

Through simulations we have verified the accuracy of our model. The value of our approach lies in its accuracy and its low computational time for the estimation of the interference mean power under varying circumstances in ad-hoc and sensor networks. Having access to interference statistics enables us to provide good estimates for the capacity of these networks.

The model presented here is a first attempt to expand the interference power sum calculation methods used in fixed topology networks to ad-hoc and sensor networks. We realize that there is room for fine-tuning and improvements in our model. One improvement, for example, is to increase the accuracy in the estimation of the standard deviation of the interference power, as discussed in Section 4.3.

Appendix

In general, the moments of r_m are:

$$E[r_m^k] = \int_0^\infty r^k \, f_{r_m}(r) \, dr = \frac{\Gamma\left(m + \frac{k}{2}\right)}{(m-1)! \, (\pi \nu)^{k/2}},$$

where $f_{r_m}(r)$ is given by (4). The variance of r_m is then:

$$Var[r_m] = E[r_m^2] - (E[r_m])^2$$

$$= \frac{1}{\pi \nu} \left(m - \left(\frac{\Gamma\left(m + \frac{1}{2}\right)}{\Gamma(m)} \right)^2 \right).$$

Using the approximation [2, 6.1.49]:

$$\frac{\Gamma\left(m + \frac{1}{2}\right)}{\Gamma(m+1)} \sim \frac{1}{\sqrt{m}} \left[1 - \frac{1}{8m} + \frac{1}{128m^2} - \cdots \right] \quad m \to \infty$$

we obtain:

$$Var[r_m] \sim \frac{1}{\pi \nu} \left(m - m \left[1 - \frac{1}{8m} + \frac{1}{128m^2} - \cdots \right]^2 \right)$$

$$\sim \frac{1}{4\pi \nu} \left(1 - \frac{1}{8m} + O\left(\frac{1}{m^2}\right) \right) \quad m \to \infty$$

From above we may conclude that the variance in the position of interfering nodes is only negligible when $\nu \gg 1$. However, the simulation results in Fig. 5 indicate that $\nu < 0.8$ for all MAC classes.

References

1. ANSI/IEEE Std 802.11, part 11: Wireless LAN medium access control (MAC) and physical layer (PHY) specifications, Tech. Rep., 1999 Edition.
2. M. Abramowitz, *Handbook of Mathematical Functions* (Dover Publications, 1970).
3. A.A. Abu-Dayya and N.C. Beaulieu, Outage probabilities in the presence of correlated lognormal interferers, IEEE Transactions on Vehicular Technology 43(1) (February 1994) 164–173.
4. C. Bettstetter and C. Hartmann, Connectivity of wireless multihop networks in a shadow fading environment, in: *Proceedings of the 6th ACM international workshop on Modeling analysis and simulation of wireless and mobile systems (MSWiM)*, San Diego, CA, USA (September 2003) pp. 28–32.
5. O. Dousse, F. Baccelli, and P. Thiran, Impact of interference on connectivity in ad hoc networks, in: *IEEE Infocom2003* (April 2003).
6. L.F. Fenton, The sum of log-normal probability distributions in scatter transmission systems, IEEE Transactions on Communications Systems 8 (March 1960) 57–67.
7. F. Graziosi and F. Santucci, Analysis of second order statistics of the SIR in cellular mobile networks, in: *50th IEEE Vehicular Technology Conference*, (September 19–22 1999) Vol. 3, pp. 1316–1320.
8. P. Gupta and P.R. Kumar, The capacity of wireless networks, IEEE Transactions on Information Theory 46(2) (March 2000) 388–404.
9. Z. Haas and J. Deng, Dual busy tone multiple access (DBTMA)—a multiple access control scheme for ad hoc networks, IEEE Transactions on Communications 50(6) (2002) 975–985.
10. R. Hekmat and P. Van Mieghem, Degree distribution and hopcount in wireless ad-hoc networks, in: *Proceeding of the 11th IEEE International Conference on Networks (ICON 2003)*, Sydney, Australia (September 28–October 1 2003) pp. 603–609.
11. R. Hekmat and P. Van Mieghem, Study of connectivity in wireless ad-hoc networks with an improved radio model, in: *Proceeding of the 2nd Workshop on Modeling and Optimization in Mobile ad hoc and Wireless Networks (WiOpt04)*, Cambridge, UK (March 28–26 2004) pp. 142–151.
12. N. Jain, S. Das, and A. Nasipuri, A multichannel MAC protocol with receiver-based channel selection for multihop wireless networks, in: *Proceedings of the 9th International Conference on Computer Communications and Networks (IC3N)* (October 2001).
13. A. Mawira, Estimate of mean C/I and capacity of interference limited mobile ad-hoc networks, in: *2002 International Zurich Seminar on Broadband Communications, Access, Transmission, Networking* (February 19–21 2002) pp. 51-1–51-6.
14. P. Pirinen, Statistical power sum analysis for nonidentically distributed correlated lognormal signals, in: *The 2003 Finnish Signal Processing Symposium (FINSIG'03)*, Tampere, Finland (May 19 2003) pp. 254–258.
15. T. Rappaport, *Wireless Communications, Principles and Practice* (Upper Saddle River Prentice-Hall PTR, 2002).
16. S.C. Schwarts and Y.S. Yeh, On the distribution function and moments of power sums with log-normal components, The Bell Systems Technical Journal 61(7) (September 1982) 1441–1462.
17. C.-K. Toh, V. Vassiliou, G. Guichal, and C.-H. Shih, MARCH: A medium access control protocol for multihop wireless ad hoc networks, in: *MILCOM 2000, 21st Century Military Communications Conference Proceedings (IEEE MILCOM)*, (October 22–25 2000) Vol. 1, pp. 512–516.
18. S.-L. Wu, Y.-C. Tseng, and J.-P. Sheu, Intelligent medium access for mobile ad hoc networks with busy tones and power control, IEEE Journal on Selected Areas in Communications 18(9) (September 2000) 1647–1657.
19. W. Ye, J. Heidemann, and D. Estrin, An energy-efficient MAC protocols for wireless sensor networks, in: *Proceedings of the IEEE Infocom 2002* (June 2002) pp. 1567–1576.

Ramin Hekmat received M.Sc. degree in electrical engineering from Delft University of Technology (TU Delft) in the Netherlands in 1990. He worked since then for several telecommunication companies in the Netherlands and the United States in Research and Development as well as managerial positions. In September 2005 he obtained Ph.D. degree for his work related to Ad-hoc Networks form TU Delft. Currently he is working as assistant professor in the faculty of Electrical Engineering, Mathematics and Computer Science of TU Delft. His prime research interest includes multi-user communication systems, wireless communications and peer-to-peer networks.

Piet Van Mieghem has obtained the Master and Ph.D. in Electrical Engineering from the K.U.Leuven (Belgium) in 1987 and 1991, respectively. He has joined the Interuniversity Micro Electronic Center (IMEC) from 1987–1991. He was a visiting scientist at MIT, department of electrical engineering from 1992-1993. From 1993 to 1998, he was working in Alcatel Corporate Research Center in Antwerp where he has gained experience in performance analysis of ATM systems and network architectural concepts of both ATM networks (PNNI) and the Internet. Currently, he is full professor at Delft University of Technology with a chair in telecommunication networks. The main theme of the research is evolution of the Internet architecture towards a broadband and QoS-aware network.